

Thiophene-based donor–acceptor conjugated polymer as potential optoelectronic and photonic material

MALUVADI G MURALI¹, UDAYAKUMAR DALIMBA^{1,*}, VANDANA YADAV²,
RITU SRIVASTAVA² and K SAFAKATH³

¹Department of Chemistry, National Institute of Technology Karnataka, Surathkal,
P.O Srinivasnagar 575 025, India

²Organic Light-Emitting Diode Laboratory, Polymeric and Soft Material Division, National Physical
Laboratory, New Delhi 110 012, India

³Light and Matter Physics Group, Raman Research Institute, C V Raman Avenue, Sadashivanagar,
Bangalore 560 080, India

e-mail: udayaravi80@gmail.com; udayakumar@nitk.ac.in

MS received 24 May 2012; revised 2 August 2012; accepted 10 August 2012

Abstract. In this paper, we report the synthesis, characterization and optical properties of a donor–acceptor conjugated polymer, **PTh-CN**, containing 3,4-didodecyloxythiophene and cyanovinylene units. The polymer possesses a low band gap of 1.75 eV as calculated from the onset absorption edge. From the electrochemical study, the HOMO and LUMO energy levels of the polymer are figured out to be -5.52 eV and -3.52 eV, respectively. Polymer light-emitting diodes are fabricated using **PTh-CN** as the emissive layer with a device configuration of ITO/PEDOT:PSS/**PTh-CN**/Al. The device showed stable saturated red electroluminescence with CIE coordinate values (0.65, 0.32) at 12 V, which are very close to the values for standard red demanded by the NTSC. In addition, the device showed good colour stability under different bias voltages and the threshold voltage of the PLED device is found to be as low as 3.1 V. Further, a nanocomposite of the polymer and TiO₂ nanoparticles is prepared by the dispersion method. The nonlinear optical properties of **PTh-CN** and **PTh-CN/TiO₂** nanocomposite are studied using z-scan technique. The polymer solution, polymer film and polymer/TiO₂ nanocomposite film show a strong saturable absorption behaviour. The value of saturation intensity (I_s) is found to be of the order 10^{11} – 10^{12} W/m², indicating that the materials are useful candidates for photonic applications.

Keywords. Conjugated polymer; cyclic voltammetry; polymer light-emitting diode; nanocomposite; NLO, z-scan.

1. Introduction

In the last two decades, a great deal of attention has been focused on the synthesis of conjugated polymers,^{1,2} because of their significant applications in the field of optoelectronic devices, such as light-emitting diodes (LEDs),³ thin film transistors,⁴ chemical sensing,⁵ photovoltaic cells,⁶ optical limiters, etc.^{7,8} In particular, electroluminescent conjugated polymers as active materials in the field of polymer light-emitting diodes (PLEDs) has attracted considerable research interest because these materials are potential candidates in flat-panel display and lighting applications. The main advantage of the conjugated polymers is the colour tunability which can be achieved by changing the mole-

cular structure of the emitting polymers by introducing suitable substituents into the polymer backbone. Hence, the design and synthesis of new conjugated polymers of varied optoelectronic properties play a vital role in the area of display technology.⁹ In this direction, donor–acceptor (D–A) conjugated polymers, introduced by Havinga *et al.*¹⁰ in the macromolecular systems via alternating electron-rich and electron-deficient substituents along a polymer backbone is the well-known approach to obtain efficient light-emitting polymers. In D–A systems, the interaction between strong electron donor (D) and strong electron acceptor (A) units in the main chain gives rise to an increased double bond character between them. Hence, a conjugated polymer with an alternating sequence of the appropriate donor and acceptor units in the main chain may show a low band gap.¹¹ Further, from the application point of view, it is necessary to develop conjugated polymers of pure blue, green and red emission colours for full colour LED

*For correspondence

devices. The cyano (CN) containing poly(2,5-dialkoxy-1,4-phenylenevinylene) (CN-DOPPV)^{12,13} and poly(3-alkylthiophene) (P3AT)^{14,15} derivatives are known to be good red light-emitting polymers. Several other red light materials have also been reported in the literature.^{16–19} Among these, thiophene derivatives are shown to be good candidates as emissive layer because of their versatility in the structural modification and good semi-conducting property.^{20,21} Since the conjugated polymers based on 3,4-dialkoxythiophene derivatives are both electron-rich and hole transporting, it is necessary to introduce electron withdrawing units to the main chains or side chains to attain lower LUMO energy level by increasing the electron affinity of the polymer. The presence of strong electron withdrawing cyano group in the polymer chain has been found to increase the electron affinity and thus enhances the electron injection and hole blocking properties of the polymer. In addition, introduction of cyanovinylene units extend the emission wavelength of the polymer to red and near infrared regions.^{18,22,23}

Further, due to the increase in effective electron delocalization along the polymer chain, the D–A conjugated polymers show large third-order nonlinear susceptibilities and hence are a promising class of third-order nonlinear materials. The strong delocalization of π -electrons in the polymeric backbone determines a very high molecular polarizability and thus remarkable third-order optical nonlinearities.^{7,24} Among various π -conjugated materials, thiophene-based polymers are currently under intensive investigation as materials for nonlinear optics because of their large third order response, chemical stability, and their readiness of functionalization. Moreover, nano-sized metal and semiconductor particles have attracted considerable interest in many areas such as optics, microelectronics, catalysis, information storage and energy conversion. They exhibit characteristic size and shape dependent electronic structures leading to unique optical and NLO properties.^{25–28} For instance, a third-order NLO susceptibility ($\chi^{(3)}$) value of 0.8×10^{-12} esu has been observed for yellow Ag colloidal nanoparticles.²⁹ Also, a large nonlinear optical response with a $\chi^{(3)}$ value as high as 2×10^{-5} esu has been observed for nanoporous layers of TiO₂.²⁸ It is advantageous to embed metal/semiconductor nanoparticles in thin polymer films for application purposes because the polymer matrix serves as medium to assemble the nanoparticles and stabilize them against aggregation.^{30,31} Moreover, nanocomposite structures are also known to enhance optical nonlinearities substantially.³² In view of these, the third-order NLO optical properties of a few metal/semiconductor-polymer

nanocomposites have been investigated.^{33–35} Further, nanocomposites using a few conjugated molecules and oligomers with metal/semiconductor nanoparticles have also been prepared. The effects of the polymer matrix on the optical properties of the nanoparticles and electronic behaviour of both the nanoparticles and conjugated materials have been investigated in these composite materials.³⁶ A nonlinear susceptibility of the order of 10^{-7} esu and an ultrafast response time of 1.2 ps has been observed for a polymer composite.³⁷ Similarly, the nanocomposite made of Ag nanoparticles dispersed in poly[2-methoxy-5-(2-ethylhexyloxy)-1,4-phenylenevinylene] matrix exhibited large third-order nonlinear susceptibility of the order of 10^{-6} esu.³⁸ Xin Chen *et al.* have observed higher $\chi^{(3)}$ value in a polydiacetylene-Ag nanocomposite film compared to pure polydiacetylene film.³⁹ However, studies on nanocomposites of donor–acceptor type conjugated polymers and metal/semiconductor nanoparticles are limited. In this context, we describe the synthesis and characterization of a donor–acceptor conjugated polymer, **PTh-CN**, containing a 3,4-didodecyloxythiophene core (donor) and a cyanovinylene linker (acceptor). Preliminary studies on the electroluminescence properties of the polymer are carried out. Further, the nonlinear optical properties of **PTh-CN** and **PTh-CN/TiO₂** nanocomposite are studied using z-scan experiment.

2. Experimental

2.1 Instrumentation

¹H NMR spectra were recorded with a BRUKER 400 MHz NMR spectrometer using TMS as internal reference. Elemental analyses were performed on a Flash EA 1112 CHNS analyzer (Thermo Electron Corporation). Infrared spectra of all the compounds were recorded on a NICOLET AVATAR 330 FTIR (Thermo Electron Corporation). UV-Vis absorption spectra were measured using a CINTRA-101 (GBC scientific equipment) spectrophotometer. The electrochemical studies of the polymer were carried out using an AUTOLAB PGSTAT 30 electrochemical analyzer. Cyclic voltammograms were recorded using a three-electrode cell system, with a glass carbon disk as working electrode, a Pt wire as counter electrode and an Ag/AgCl electrode as the reference electrode with 0.1 M tetrabutylammoniumperchlorate (TBAPC)/CH₃CN as the electrolyte at a scan rate of 50 mV/s at room temperature. Fluorescence spectra were recorded using a JASCO FP6200 spectrofluorometer. Gel permeation chromatography (GPC) was used

to obtain the molecular weight of the polymer and was determined by Waters make GPC instrument with reference to polystyrene standards with THF as eluent. Polymer and nanocomposite films are prepared using an ACE -1020 (Dong Ah Trade & Tech. Corp.) spin coating unit. The EL spectrum was determined using HR 2000 Ocean Optics spectrometer, having a CCD array and fibre optic probe. The current-voltage characteristic of the PLED devices was studied using a Keithley 2400 programmable digital source meter. The thickness of the deposited layers was measured by ellipsometry. Thermogravimetric analysis was carried out using an EXSTAR TG/DTA 7000 (SII Nanotechnology Inc.) thermal analyzer. SEM images are obtained with a CARL ZEISS SUPRA 40 VP (NTS GmbH Germany) field emission scanning electron microscopy (FESEM).

2.2 Materials

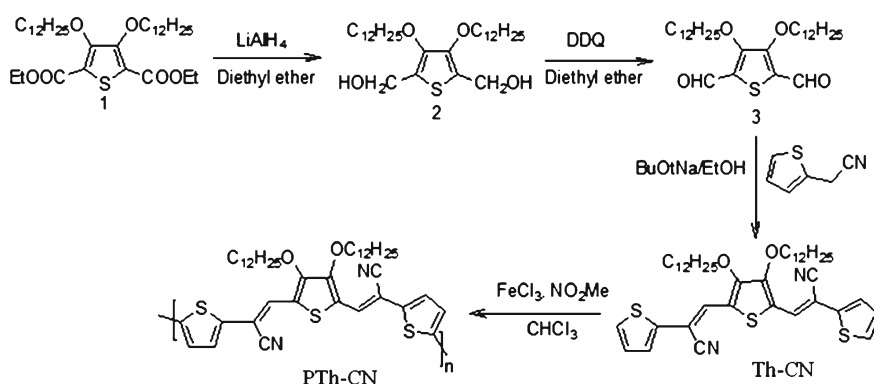
Diethyl 3,4-didodecyloxythiophene-2,5-dicarboxylate (1) was prepared according to the previously reported method.⁴⁰ Lithium aluminum hydride, 2,3-dichloro-5,6-dicyano benzoquinone, thiophene-2-acetonitrile, sodium tert-butoxide, poly(3,4-ethylene dioxythiophene):poly(styrene sulphonate) (PEDOT:PSS) and nano-sized TiO₂ powder were purchased from Sigma Aldrich Chemical Co. Tetrabutylammoniumperchlorate (TBAPC) was purchased from Lancaster company (UK). All solvents and other reagents were purchased commercially and used without further purification.

2.3 Synthesis of monomer (Th-CN) and polymer (PTh-CN)

The synthetic route for preparing the monomer and the polymer are depicted in scheme 1. The detailed synthetic procedures for the synthesis of the monomer and the polymer are as follows.

2.3a Synthesis of (3,4-bis(dodecyloxy)thiophene-2,5-diyl)dimethanol (2): To a solution of diethyl 3,4-didodecyloxythiophene-2,5-dicarboxylate, **1**, (1 g, 1.67 mmol) in 10 ml of dry diethyl ether, 0.15 g (4.18 mmol) lithium aluminum hydride (LiAlH₄) was added at 0°C. The reaction mixture was stirred at room temperature for 1 h. After completion of reaction (monitored by TLC), the resulting mixture was quenched with saturated NH₄Cl solution. The residue obtained was filtered through celite and was washed with dichloro methane. The filtrate thus obtained was washed with water, dried with MgSO₄ and concentrated to get the product as white solid in 80% yield. M.P: 72–73°C. ¹H NMR (400 MHz, CDCl₃, δ, ppm): 4.72 (s, 4H, -CH₂OH), 4.02 (t, J = 6.4 Hz, 4H, -OCH₂), 1.80–1.26 (m, 40H, -(CH₂)₁₀-), 0.88 (t, J = 6.8 Hz, 6H, -CH₃). FTIR, √ (cm⁻¹): 3311 (-OH), 2915 and 2848 (-C-H), 1500, 1462, 1427, 1364, 1240, 1086, 992. Element. Anal. Calcd. For C₃₀H₅₆O₄S: C, 70.26; H 11.01; S, 6.24; found: C, 70.28; H, 11.04; S, 6.22.

2.3b Synthesis of 3,4-bis(dodecyloxy)thiophene-2,5-dicarbaldehyde (3): To a solution of compound **2** (0.5 g, 0.97 mmol) in 5 ml of dry diethyl ether, 0.66 g (2.29 mmol) 2,3-dichloro-5,6-dicyanobenzoquinone (DDQ) was added portion-wise at room temperature. The reaction mixture was stirred at room temperature for 72 h. After completion of the reaction (monitored by TLC), the solvent was evaporated. The solid residue obtained was redissolved in 50 ml *n*-hexane and filtered off. The organic layer was washed with water several times, dried with MgSO₄ and concentrated. Finally, the obtained crude solid product was recrystallized with ethanol to get the product as white crystals in 60% yield. M.P: 52–54°C. ¹H NMR (400 MHz, CDCl₃, δ, ppm): 10.09 (s, 2H, -CHO), 4.26 (t, J = 6.4 Hz, 4H, -OCH₂), 1.83–1.26 (m, 40H, -(CH₂)₁₀-), 0.88 (t, J = 6.8 Hz, 6H, -CH₃). FTIR, √ (cm⁻¹): 2914 and 2848



Scheme 1. Synthetic route of the monomer and the polymer.

(-C-H), 1656 (-C=O), 1480, 1430, 1366, 1263, 1186, 1037, 798. Element. Anal. Calcd. For $C_{30}H_{52}O_4S$: C, 70.82; H, 10.31; S, 6.29; found: C, 70.80; H, 10.34; S, 6.26.

2.3c Synthesis of 3,3'-(3,4-bis(dodecyloxy)thiophene-2,5-diyl)bis(2-(thiophen-2-yl)acrylonitrile) (Th-CN): To a stirred solution of dialdehyde **3** (1 g, 1.96 mmol) and thiophene-2-acetonitrile (0.5 g, 4.12 mmol) in 10 ml absolute ethanol under argon, a solution of 0.56 g of sodium tert-butoxide (5.89 mmol) in 5 ml of absolute ethanol was added through a syringe. The mixture was stirred at room temperature for 2 h. The precipitated solid was filtered off to give dark red shiny solid in 70% yield. M.P: 89°C. 1H NMR (400 MHz, $CDCl_3$, δ , ppm): 7.57 (s, 2H, -olefinic proton-), 7.37–7.35 (dd, $J_1 = 1.2$ Hz, 2H, $J_2 = 3.6$ Hz), 7.30–7.28 (dd, $J_1 = 1.2$ Hz, $J_2 = 5.2$ Hz, 2H), 7.07–7.05 (dd, $J_1 = 4$ Hz, $J_2 = 5.2$ Hz, 2H), 4.11 (t, 4H, -OCH₂-), 1.80–1.26 (m, 40H, -(CH₂)₁₀-), 0.88 (t, 6H, -CH₃). FTIR, $\sqrt{}$ (cm^{-1}): 2913 and 2845 (-C-H), 2205 (-CN), 1568, 1454, 1377, 1282, 1159, 1013, 946. Element. Anal. Calcd. For $C_{42}H_{58}N_2O_2S_3$: C, 70.16; H, 8.14; N, 3.90; S, 13.35; found: C, 70.12; H, 8.12; N, 3.86; S, 13.38.

2.3d Synthesis of polymer (PTh-CN): To a stirred solution of monomer **Th-CN** (500 mg, 0.695 mmol) in 50 ml of chloroform was added anhydrous $FeCl_3$ (0.56 g, 3.47 mmol) in nitromethane drop-wise over a period of 45 min at room temperature under argon atmosphere. The light red monomer solution turned progressively dark violet with addition of oxidizing agent. The mixture was stirred for 24 h and then added into methanol (200 ml). The precipitate was filtered, dissolved in $CHCl_3$, and extracted with water. Solvent was removed and the residue was redissolved in chloroform (50 ml) and hydrazine monohydrate (25 ml). To reduce the polymer to neutral form, the mixture was stirred for 12 h. After evaporation of $CHCl_3$, the residue was precipitated in methanol (200 ml) and filtered off. Then the residue was stirred in acetone to remove unreacted monomers. The polymer was filtered and dried under vacuum to give polymer (**PTh-CN**) as violet solid. 1H NMR (400 MHz, $CDCl_3$, δ , ppm): 7.57 (s, 2H, -olefinic proton-), 7.35 (d, $J = 3.6$ Hz, 2H), 7.14 (d, $J = 4$ Hz, 2H), 4.13 (t, 4H, -OCH₂-), 1.83–1.23 (m, 40H, -(CH₂)₁₀-), 0.87 (t, 6H, -CH₃). FTIR, $\sqrt{}$ (cm^{-1}): 2912 and 2846 (-C-H), 2206 (-CN), 1567, 1451, 1368, 1260, 1024, 785, 684. Element. Anal. Calcd. For $C_{42}H_{56}N_2O_2S_3$: C, 70.36; H, 7.88; N, 3.91; S, 13.39; found: C, 70.28; H, 7.76; N, 3.84; S, 13.48.

2.4 Fabrication of the polymer light-emitting diode devices

In the device fabrication, we used the simplest sandwich structure for the device configuration with poly(3,4-ethylenedioxythiophene):poly(styrenesulphonate) (PEDOT:PSS) coated indium tin oxide (ITO) glass as the anode, the spin coated polymer (**PTh-CN**) as the emissive layer and aluminum as the cathode. To fabricate PLEDs of device configuration ITO/PEDOT:PSS/**PTh-CN**/Al, first the indium tin oxide (ITO) coated glass substrates with a sheet resistance of 20 Ω /square and a thickness (ITO) of 120 nm were cleaned using deionized water, acetone, trichloroethylene and isopropyl alcohol sequentially for about 20 min each using an ultrasonic bath and dried in vacuum oven. Then ITO surface was treated with oxygen plasma for about 5 min to increase its work function. Then, a hole injection layer of PEDOT:PSS was spin coated on the cleaned and patterned ITO substrates at 4000 rpm with about 50–60 nm in thickness and was dried by baking at 120°C in vacuum for \sim 1 h. Then, the emitting layer, **PTh-CN**, was spin cast onto the PEDOT:PSS layer at a speed of 2000 rpm from chlorobenzene solution (10 mg/mL) through a 0.45 μ m teflon filter, followed by vacuum annealing at 150°C for \sim 2 h in order to remove the organic fraction. Finally, the coated ITO was transferred to a deposition chamber, where a layer of Al electrodes was vacuum deposited on the polymer layer with about 200 nm in thickness by thermal evaporation at a pressure of 1×10^{-6} Torr. Four pixels, each of active area of 4×4 mm² are defined per substrate and were used to assess the reproducibility of the device performance. The complete fabricated devices were finally annealed at 100°C in vacuum for 5 min before being characterized. All the characterization of the light-emitting diode device was carried out at room temperature under ambient conditions without protective encapsulation.

2.5 Preparation of PTh-CN/TiO₂ nanocomposite films

For the preparation of polymer nanocomposite (**PTh-CN/TiO₂**) films, 10 weight% TiO_2 nanoparticles were dispersed in the polymer using chloroform and chlorobenzene solvent system (10:1 volume ratio) and sonicated for 2 h. Nanocomposite films are prepared on clean glass plates by spin coating and the films are dried under vacuum for 1 h.

2.6 Z-Scan measurements

The z-scan technique is a widely used method developed by Sheik Bahae *et al.*⁴¹ to measure the nonlinear

absorption coefficient and nonlinear refractive index of materials. The ‘open aperture’ z-scan gives information about the nonlinear absorption coefficient. A nearly Gaussian laser beam is used for optically exciting the sample, and its propagation direction is considered as the z-axis. The beam is focused using a convex lens and the focal point is taken as $z = 0$. Obviously, the beam will have maximum energy density at the focal point, which will symmetrically reduce towards either side of it, for the positive and negative values of z . In the experiment the sample is placed in the beam at different positions with respect to the focus (i.e., at different values of z), and the corresponding optical transmission values are measured. Then a graph is plotted between z and the measured sample transmission (normalized to its linear transmission), which is known as the z-scan curve. The shape of the z-scan curve will provide information on the nature of the nonlinearity. The nonlinear absorption coefficient of sample can be calculated by fitting the experimental data to theory.

In our z-scan experiment, we have used a stepper-motor controlled linear translation stage, to move the sample through the beam in precise steps. Two pyroelectric energy probes (Rj7620, Laser Probe Inc.) are used to measure the transmission of the sample at each point. One energy probe monitors the input energy, while the other monitors the transmitted energy through the sample. The second harmonic output (532 nm) of a Q-switched Nd:YAG laser (Minilite-Continuum, 5 ns FWHM laser pulses) was used for excitation of samples. The linear transmissions of the samples studied were in the range of 50% to 75% at 532 nm. The experiments were carried out in the ‘single shot’ mode, allowing sufficient time between successive pulses to avoid accumulative thermal effects in the sample. The experiment was automated, controlled by a data acquisition program written in Lab VIEW.

3. Results and discussion

3.1 Synthesis and characterization

The synthetic method followed for the synthesis of monomer **Th-CN** and polymer **PTh-CN** is depicted in scheme 1. 3,4-Bis(dodecyloxy)thiophene-2,5-dicarbaldehyde (**3**) was synthesized starting from diethyl 3,4-didodecyloxythiophene-2,5-dicarboxylate (**1**). The diester compound (**1**) was reduced using lithium aluminum hydride in ether at room temperature to obtain (3,4-bis(dodecyloxy)thiophene-2,5-diyl)dimethanol (**2**). The bisalcohol (**2**) was then oxidized to the dicarbaldehyde (**3**), using 2,3-dichloro-5,6-dicyano-1,4-benzoquinone as the oxidizing agent. In the next step,

a Knoevenagel condensation reaction was performed between 3,4-bis(dodecyloxy)thiophene-2,5-dicarbaldehyde (**3**) and thiophene-2-acetonitrile in ethanol in the presence of sodium tert-butoxide under argon atmosphere to yield the monomer, **Th-CN**. The overall yields for all the intermediate compounds were between 60 and 80%. Polymer **PTh-CN** was prepared by the chemical oxidation of the monomer (**Th-CN**) using FeCl_3 as oxidizing agent. This method is very useful to prepare polythiophenes due to its simplicity and the high molecular weights achieved. After the polymerization reaction, the residual iron (III) salts present in the mixture were reduced in concentration with rigorous purification. The crude polymer obtained was precipitated with methanol several times in order to remove residual FeCl_3 . The oxidative polymerization reaction gives the polymer in the oxidized (doped) form. The reduction (dedoping) of the polymer was achieved using hydrazine to get the polymer in the neutral form. Further, the polymer was stirred with acetone so as to remove any traces of unreacted monomer. All the intermediate compounds and the polymer showed good solubility in common organic solvents, such as CHCl_3 , THF and chlorobenzene, resulting from the alkoxy chains at 3 and 4-positions of the thiophene ring. The chemical structures of all the intermediate compounds and the polymer were confirmed by ^1H NMR spectroscopy, FTIR spectroscopy and elemental analysis. The ^1H NMR spectrum of monomer **Th-CN** showed a singlet at δ 7.57 ppm which is assigned to the olefinic protons. The three double doublet peaks in the range of δ 7.37–7.35, 7.07–7.05 and 7.30–7.28 ppm are assigned to thiophene ring protons at position 2, 3 and 4, respectively. The triplet peak at δ 4.11 ppm is due to $-\text{OCH}_2-$ protons of the alkoxy chains of the thiophene ring and the multiple peaks in the range δ 1.80–0.88 ppm are due to $-(\text{CH}_2)_{10}-\text{CH}_3$ protons of the alkoxy chains. Polymerization of the monomer **Th-CN** was confirmed by the ^1H NMR spectrum. In the ^1H NMR spectrum, the disappearance of double doublet peak of thiophene ring proton at position 2 and conversion of double doublet in to a doublet peak gave a clear evidence of successful polymerization of the monomer to the polymer. The ^1H NMR spectrum of polymer **PTh-CN** showed a singlet at δ 7.57 ppm due to olefinic protons. The two doublet peaks at δ 7.35 and 7.14 ppm are assigned to thiophene ring protons at positions 3 and 4, respectively. A triplet peak at δ 4.13 ppm is due to the $-\text{OCH}_2-$ protons of the alkoxy chains of the thiophene ring and the multiple peaks in the range 1.83–0.87 ppm are due to the $-(\text{CH}_2)_{10}-\text{CH}_3$ protons of the alkoxy chains. The average molecular weights of the polymer were measured by gel permeation chromatography (GPC) with

reference to polystyrene standards. The number averaged molecular weight (M_n) of the polymer is found to be 15800 and the molecular weight distribution (PDI) is 2.1. Generally, the chemical polymerization method gives polymers with high molecular weights. But, the average molecular weights of **PTh-CN** are rather low. This could be due to the presence of strong electron withdrawing cyano group in the monomer, which deactivates thiophene ring towards oxidative polymerization reaction. This effect becomes more prominent in the growing polymer chain due to increase in the number cyano groups with successive addition of the repeating units. As a result, further addition of monomeric units becomes difficult which terminates the polymerization process. Hence a low molecular weight polymer sample is obtained in the present study. The strong bands at 2912 and 2846 cm^{-1} in the FTIR spectrum of **PTh-CN** are due to (C–H) stretching vibrations of the alkyl chains. The band at 2206 cm^{-1} is assigned to the $\text{C}\equiv\text{N}$ stretching vibration. FTIR spectrum of the TiO_2 nanoparticles exhibits a band at 3397 cm^{-1} due to O–H stretching mode of Ti–OH. The characteristic absorption band of Ti–O–Ti was observed at 475 cm^{-1} .⁴² All these characteristic bands arising from both TiO_2 nanoparticles and **PTh-CN** were observed in the spectrum of **PTh-CN/TiO₂** nanocomposite, confirming the incorporation of TiO_2 nanoparticles in the nanocomposite structure.⁴³ Smooth and optically clear thin solid films on glass substrates were obtained by spin-coating the chloroform solutions of the polymer (1 mg mL^{-1}) at a spin rate of 1500 rpm. Figure 1 shows the FESEM image of the **PTh-CN/TiO₂** nanocomposite. A moderately uniform distribution of TiO_2 nanoparticles was observed with average particle sizes ranging from 25 to 50 nm. The thickness of polymer films and nanocom-

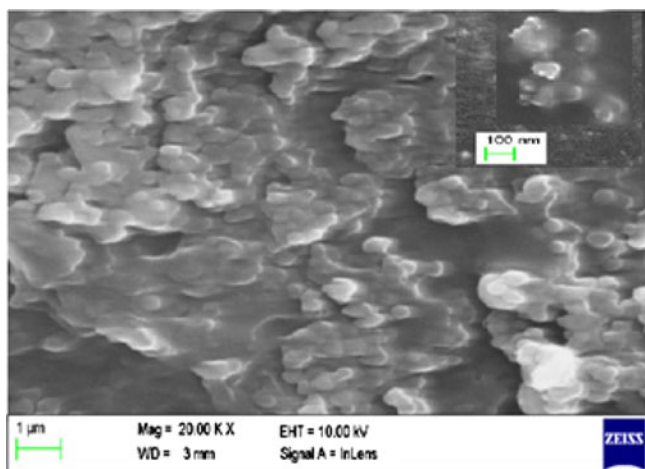


Figure 1. FESEM images of **PTh-CN/TiO₂** nanocomposite (inset: magnified image, Mag = 100 KX).

posite films were determined by SEM cross section and was found to be in the range 0.9–1 micrometer.

3.2 UV-Vis absorption studies

The UV-Vis absorption spectra could provide a good deal of information on the electronic structure of conjugated polymers. Figure 2 shows the absorption spectra of monomer **Th-CN** and polymer **PTh-CN** in dilute chloroform solution along with the spectra of **PTh-CN** thin film and **PTh-CN/TiO₂** nanocomposite thin film. The monomer solution displayed an absorption maximum at 457 nm, whereas for the polymer solution an absorption maximum is observed at 550 nm. The monomer being a donor–acceptor conjugated molecule shows absorption in the visible region. The presence of alternating electron withdrawing and electron releasing units in a conjugated system results in strong intramolecular charge transfer (ICT) interactions, which extends the absorption to longer wavelength regions. The polymer thin film, in addition to an absorption maximum at 550 nm, showed a peak in the shorter wavelength region at 390 nm and a shoulder at 661 nm. The optical energy band gap (E_g) of **PTh-CN** is found to be 1.75 eV in the thin film state. The broadening of the absorption spectrum of the polymer film in comparison with that of the polymer solution could be due to the enhanced interchain interaction in the solid film state and increased polarizability of the film. The absorption spectra of **PTh-CN/TiO₂** nanocomposite thin film showed a red shift of about 18 nm in comparison with that of the polymer film. The observed

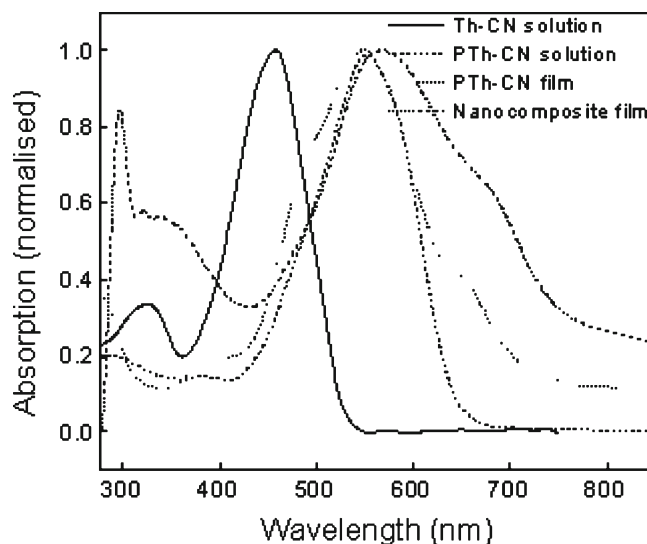


Figure 2. UV-Vis absorption spectra of **Th-CN** solution, **PTh-CN** in chloroform solution, **PTh-CN** thin film and **PTh-CN/TiO₂** nanocomposite thin film.

Table 1. Linear optical and nonlinear optical properties of the polymer.

	Linear optical properties λ_{\max} (nm)				Nonlinear optical properties (z- scan) I_s in W/m ²		
	Solution ^a	Film ^b	Nanocomposite film ^b	E_g^{opt} eV	Solution ^a	Film ^b	Nanocomposite film ^b
PTh-CN	550	550	568 (295)	1.75	2×10^{12}	6×10^{11}	9×10^{11}

^aMeasured in chloroform solution. ^b Cast from chloroform solution

E_g^{opt} , Bandgap estimated from the onset wavelength of the optical absorption of the polymer film

I_s Saturation intensity measured from z-scan technique

red shift in the absorption maximum can be understood in terms of enhanced effective π -conjugation length in **PTh-CN/TiO₂** nanocomposite film as compared to that of **PTh-CN** film. A similar trend in the absorption maximum was observed for MEH-PPV/TiO₂ nanocomposite films.⁴⁴ Further, the peak observed at 295 nm in the nanocomposite film is assigned to the characteristic absorptions of TiO₂ nanoparticles. These optical results indicate that some interactions occur between the conjugated polymer chains and TiO₂ nanoparticles. The optical properties of **PTh-CN** are summarized in table 1.

3.3 Thermal stability

The thermal property of polymer **PTh-CN** and **PTh-CN/TiO₂** nanocomposite were determined by thermogravimetric analysis (TGA) and was carried out under nitrogen atmosphere at a heating rate of 10°C/min. The TGA reveals that, both the polymer and the nanocomposite possess good thermal stability. The onset decomposition temperature for the polymer was observed near 180°C with a gradual weight loss until 320°C, which could be attributed to the loss of alkoxy or alkyl chains present on the thiophene ring. Beyond this temperature range, the weight loss increases abruptly, indicating the decomposition of the polymer backbone. The nanocomposite is thermally stable up to 300°C. When the temperature is increased beyond 300°C, there is a sharp weight loss near 350°C and it continues until 650°C. Similar trend was observed for other nanocomposites reported in the literature.⁴³ These results indicate that there is a strong interaction exists at the interface of the polymer and TiO₂ nano particles in the nanocomposite structure.

3.4 Electrochemical properties

The device fabrication and investigation of LED characteristics of polymers require information on the electronic structure of the luminescent polymer

which can be determined by electrochemical studies. Cyclic voltammetry was used to investigate the redox behaviour of the polymer and to assess the HOMO and LUMO energy levels. All measurements were calibrated with the ferrocene/ferrocenium (Fc/Fc⁺) standard ($E_{\text{FOC}} = 0.53$ vs. Ag/AgCl). As shown by the cyclic voltammogram in figure 3, the polymer showed both *n*-doping and *p*-doping processes. On sweeping the polymer cathodically, the onset of the *n*-doping process occurred at a potential value of -0.75 V with a reduction peak at -1.06 V. In the anodic scan, the *p*-doping onset was observed at 1.25 V followed by an oxidation peak at 1.55 V. The onset potentials of *n*-doping and *p*-doping processes were used to estimate the HOMO and LUMO energy levels of the conjugated polymer according to the equations,⁴⁵

$$E_{\text{HOMO}} = -[E_{(\text{onset})}^{\text{ox}} + 4.8 \text{ eV}] \text{ and}$$

$$E_{\text{LUMO}} = -[E_{(\text{onset})}^{\text{red}} + 4.8 \text{ eV}],$$

where $E_{(\text{onset})}^{\text{ox}}$ and $E_{(\text{onset})}^{\text{red}}$ are the onset potentials for the oxidation and reduction processes of a polymer, respectively. Accordingly, the HOMO and LUMO energy

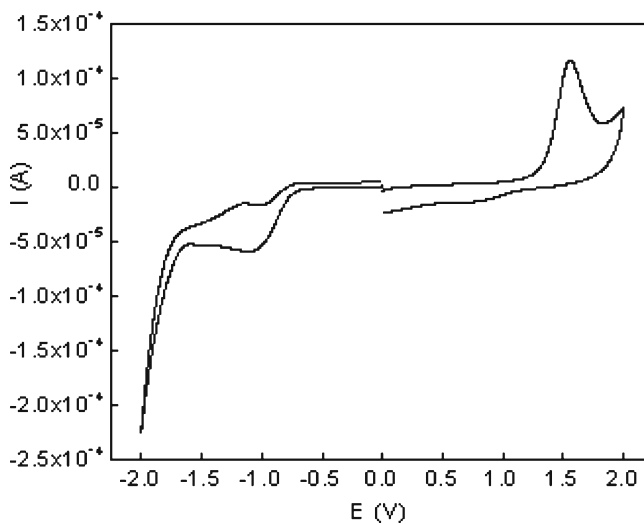


Figure 3. Cyclic voltammogram of the polymer film cast on glassy carbon disk in 0.1 M tetrabutylammoniumperchlorate (TBAPC)/CH₃CN solution at 50 mV/s.

Table 2. Electrochemical properties of the polymer.

Polymer	$E_{(\text{onset})}^{\text{ox}}$ (V)	$E(\text{oxd})$ (V)	$E_{(\text{onset})}^{\text{red}}$ (V)	$E(\text{red})$ (V)	HOMO (eV)	LUMO (eV)	E_g (eV)
PTh-CN	1.25	1.55	-0.75	-1.06	-5.52	-3.52	2.0

E_g^{Ec} Electrochemical band gap estimated from the difference between E_{HOMO} and E_{LUMO}

levels of the polymer are estimated to be -5.52 eV and -3.52 eV, respectively and hence electrochemical band gap of the polymer is 2.0 eV. The electrochemical band gap of the polymer is higher than the optical band gap. This difference is due to the creation of free ions in the electrochemical experiment compared with the one measured through UV experiments, which refers to a neutral state. From the high electron affinity value, which could be attributed to the electron withdrawing property of $-\text{CN}$ units in the polymer backbone, it can be expected that the polymer may show increased electron injection ability in PLEDs. Also, the electrochemical data support the argument that the injection of electrons and holes would be more balanced in the polymer. The cyclic voltammetry data of the polymer are summarized in table 2.

3.5 Fluorescence emission and electroluminescence properties

Fluorescence emission studies of **Th-CN** and **PTh-CN** reveal that **Th-CN** and **PTh-CN** in dilute chloroform solution emit intense green and red light, respectively, under the irradiation of UV light with emission maxima at 550 nm for **Th-CN** and 657 nm for **PTh-CN**. The fluorescence quantum yield (ϕ_{fl}) of the polymer in chloroform solution was estimated by comparing with the standard of quinine sulphate (ca. 1×10^{-5} M solution in 0.1 M H_2SO_4 having a fluorescence quantum yield of 55%).⁴⁶ The quantum yield of the polymer is 38%.

PLED devices fabricated with a configuration of ITO/PEDOT:PSS/**PTh-CN**/Al were used to investigate the electroluminescent (EL) behaviour of the polymer (**PTh-CN**) as emissive material for polymer light emitting diodes. The devices are fabricated under ambient conditions and are characterized without using any protective encapsulation. The EL spectra of polymer **PTh-CN** under different driving voltages ranging from 7 V to 14 V are as shown in figure 4. The EL spectra show that with an increase in the applied voltage, the intensity of the emitted light also increases as a function of wavelength. The PLED devices emitted red light with emission maxima originated at 615 and 670 nm. Also, the EL spectrum of the polymer showed stable red emission without any considerable spectral change and/or

additional peaks with driven voltage. The EL spectra of the polymer was blue shifted relative to the corresponding PL spectra which results from different exciton generation processes and heating of the LEDs because of applied voltages during the measurement. This suggests that the local heating in the polymer film at high voltages probably leads to conformational changes of the polymer backbone. The colour stability under different voltages for **PTh-CN** was also investigated. The CIE coordinates of the polymer devices under different voltages of 11 V, 12 V, 13 V and 14 V were (0.64, 0.32), (0.65, 0.32), (0.66, 0.32) and (0.64, 0.32), respectively. The EL peak position and the CIE coordinates of the device were not changed significantly under different driving voltages. These results indicate that the polymer show good colour stability under different applied voltages. The colour coordinates of the red emitting **PTh-CN** is closer to the standard red (0.66, 0.34) demanded by the National Television System Committee (NTSC) indicating that **PTh-CN** emits almost pure red colour.⁴⁷ The current density-voltage characteristics of the PLED device (figure 5) show that the current density of the polymer increases exponentially with the increasing forward bias voltage, which is a typical diode characteristic. The polymer shows low threshold voltage of 3.1 V. The lower threshold voltage can be attributed to the lower energy barrier for electron injection (due to

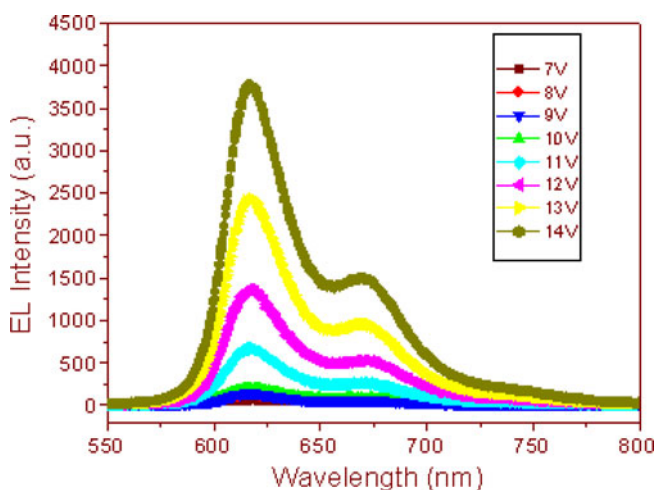


Figure 4. Electroluminescence (EL) spectra of the ITO/PEDOT:PSS/**PTh-CN**/Al device at varying forward applied voltages.

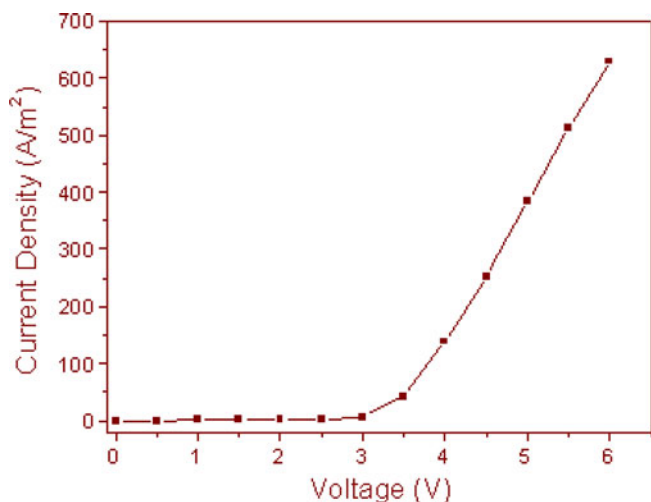


Figure 5. Current density-voltage characteristics of the ITO/PEDOT: PSS/ PTh-CN/Al device.

low lying LUMO level of the polymer) from the aluminum electrode. The low threshold voltage value can be comparable with some of the previously reported light-emitting polymers which showed good EL performance.²³ These preliminary studies on EL properties of PTh-CN suggest that the polymer may be used for the fabrication of stable red light-emitting diodes.

3.6 Nonlinear optical properties

The open aperture z-scan curves obtained in the polymer PTh-CN solution, PTh-CN film and PTh-CN/TiO₂ film are shown in figures 6, 7 and 8, respectively. The laser pulse energies used to excite the samples were between 10 and 100 μ J. All samples show a pure saturable absorption (SA) behaviour.

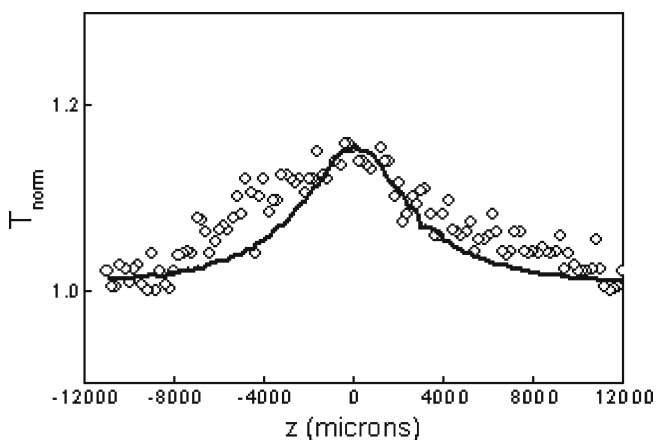


Figure 6. Open aperture z-scan of PTh-CN in solution having a linear transmission of 51% at 532 nm. The laser pulse energy is 100 μ J. Circles are data points while the solid curve is a numerical fit according to Eq. 1.

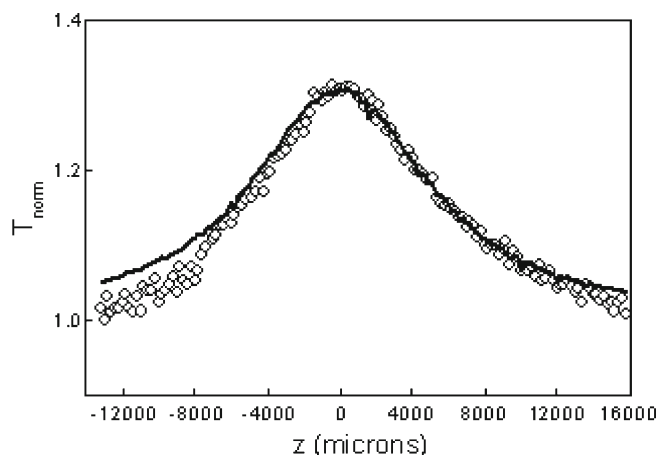


Figure 7. Open aperture z-scan of PTh-CN film having a linear transmission of 72% at 532 nm. The laser pulse energy is 10 μ J. Circles are data points while the solid curve is a numerical fit according to Eq. 1.

Saturable absorption is a property of a material where the absorption of light decreases with the increase of light intensity. At sufficiently high incident light intensity, atoms or molecules in the ground state of a saturable absorber material become excited into upper energy state at such a rate that there is insufficient time for them to decay back to the ground state before the ground state becomes depleted, and the absorption subsequently saturates. In a saturable absorber, the nonlinear absorption coefficient α is given by,

$$\alpha = \alpha_0 \frac{1}{1 + \left(\frac{I}{I_s}\right)}, \quad (1)$$

where α_0 is the linear absorption coefficient at the wavelength of excitation, I is the incident intensity,

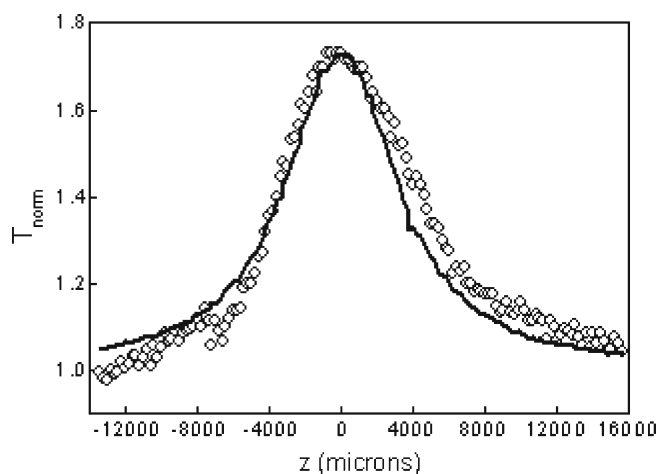


Figure 8. Open aperture z-scan of PTh-CN/TiO₂ film having a linear transmission of 50% at 532 nm. The laser pulse energy is 10 μ J. Circles are data points while the solid curve is a numerical fit according to Eq. 1.

and I_s is the saturation intensity. The z-scan profile usually shows a valley with a maximum and a minimum on each side of the focal point. However, in our study, the open aperture z-scan profile shows a typical peak, symmetric about the focus, which is known to be the signature of saturable absorption behaviour. The peak appears at the focal point where the laser pulse has the strongest fluence. A similar type of saturable absorption in the near-field transmission was observed for inorganic materials.⁴⁸ The z-scan curves obtained are fitted with numerically simulated results using Eq. (1). By determining the best-fit curves for the experimental data, the nonlinear parameters could be calculated. For **PTh-CN** solution, saturation intensity (I_s) was found to be 2×10^{12} W/m², for **PTh-CN** film it was 6×10^{11} W/m² and for **PTh-CN/TiO₂** nanocomposite film it was found to be 9×10^{11} W/m². Obviously there is an enhancement of nonlinearity in **PTh-CN/TiO₂** nanocomposite film compared to pure **PTh-CN** film. This is not substantial though, the reason being that the polymer films themselves are highly nonlinear in nature. From a device point of view both **PTh-CN** and **PTh-CN/TiO₂** nanocomposite films are equally useful. Because of their large saturable absorption, both **PTh-CN** and **PTh-CN/TiO₂** nanocomposite films are expected to be useful candidates for photonic applications mainly in the areas such as Q-switching and mode-locking of lasers, pulse shaping, and optical switching.⁴⁹ For comparison, similar saturable absorption behaviour is observed for some organic materials in the literature. The values of I_s obtained are 1.5 to 4.5×10^{13} W/m² in phthalocyanines, 1 to 4×10^{10} W/m² in poly(indenofluorene), 10^{10} to 10^{11} W/m² for Rhodamine B and 1.4 to 6.8×10^{13} W/m² for thiophene-based conjugated polymers.^{50–53} The value of I_s obtained for **PTh-CN** is almost 100 times lower than the values obtained for thiophene-based donor–acceptor polymers,⁵³ indicating a better NLO response in **PTh-CN**. This could be due to the presence of stronger electron withdrawing cyano group in **PTh-CN** in comparison with 1,3,4-oxadiazole groups in the reported polymers. The nonlinear optical properties of the polymer are summarized in table 1. The presence of strong electron donor and electron acceptor groups in the polymer chain increases π -electron delocalization and hence improves the NLO properties of the polymer. Thus, incorporation of cyano groups as electron acceptors in donor–acceptor conjugated polymers could be a promising molecular design to achieve high NLO responses in polymers. Further, nanocomposite structures formed by the incorporation of **TiO₂** nanoparticles into the polymer matrix found to enhance the NLO properties of the polymer. Hence donor–acceptor con-

jugated polymers and their nanocomposites could be potential candidates for photonic applications.

4. Conclusions

A donor–acceptor type conjugated polymer, **PTh-CN** containing 3,4-didodecyloxythiophene unit as electron donor moiety and cyanovinylene unit as electron acceptor moiety was synthesized and characterized. The push–pull (D–A) arrangement along with the presence of strong electron withdrawing cyano group in the polymer structure greatly influenced its electronic structure. Hence the polymer showed a lower bandgap with a low-lying LUMO energy level. As a result, the polymer light-emitting device based on **PTh-CN** showed a low threshold voltage of 3.1 V indicating an efficient electron injection in the device. Further, the polymer device showed almost pure red emission with a CIE coordinate of (0.65, 0.32), which is very close to the standard red. Also, the device, without any protective encapsulation, showed good colour stability under different bias voltages. The **PTh-CN/TiO₂** nanocomposite was prepared using the dispersion method. Incorporation of **TiO₂** nanoparticles into the polymer matrix found to improve the thermal stability of the polymer. The nonlinear optical properties of **PTh-CN** and **PTh-CN/TiO₂** nanocomposite are studied using z-scan technique. All the samples show a strong saturable absorption behaviour and the incorporation **TiO₂** nanoparticle marginally enhances the nonlinear optical property in **PTh-CN/TiO₂** nanocomposite film when compared to the pure **PTh-CN** film. The NLO results signify that the materials are useful candidates for photonic applications.

Supplementary information

The electronic supporting information can be seen in www.ias.ac.in/chemsci.

Acknowledgements

Authors from the National Institute of Technology Karnataka (NITK) thank Dr. Reji Philip, Raman Research Institute (RRI), Bangalore for providing facility for z-scan studies.

References

1. Skotheim T A, Elsenbaumer R L and Reynolds J R 1998 *Handbook of conducting polymers* (New York: Marcel-Dekker)

2. Mullen K and Wegner G 1998 *Electronic materials, the oligomer approach* (Weinheim, Germany: Wiley-VCH)
3. Burroughes J H, Bradley D D C, Brown A R, Marks R N, Mackay K, Friend R H, Burn P L and Holmes A B 1990 *Nature* **347** 539
4. Li Y, Wu Y and Ong B S 2006 *Macromolecules* **39** 6521
5. McQuade D T, Pullen A E and Swager T M 2000 *Chem. Rev.* **100** 2537
6. Yu G, Gao J, Hummelen J C, Wudl F and Heeger A J 1995 *Science* **270** 1789
7. Prasad P N and David J W 1991 *Introduction to non-linear optical effects in molecules and polymers* (New York: Wiley)
8. Kishino S, Ueno Y, Ochiai K, Rikukawa M, Sanui K, Kobayashi T, Kunugita H and Ema K 1998 *Phys. Rev. B.* **58** 13430
9. Choi M C, Kim Y and Ha C S 2008 *Prog. Polym. Sci.* **33** 581
10. Havinga E E, Hoeve W and Wynberg H 1993 *Synth. Met.* **55** 299
11. Colladet K, Fourier S, Cleji T J, Laurence L, Gelan J and Vanderzande D 2007 *Macromolecules* **40** 65
12. Greenham N C, Moratti S C, Bradley D D C, Friend R H and Holmes A B 1993 *Nature* **365** 628
13. Liu Y, Yu G, Li Q and Zhu D 2001 *Synth. Met.* **122** 401
14. Berggren M, Inganäs O, Gustafsson G, Rasmussen J, Andersson M R, Hjertberg T and Wennerström O 1994 *Nature* (London) **372** 444
15. Andersson M R, Berggren M, Inganäs O, Gustafsson G, Gustafsson-Carberg J C, Selece D, Hjertberg T and Wennerström O 1995 *Macromolecules* **28** 7525
16. Cho N S, Park J H, Lee S K, Lee J and Shim H K 2006 *Macromolecules* **39** 177
17. Chen C H, Klubek K P and Shi J 1999 *U.S. Patent* 5908581
18. Kim J H and Lee H 2002 *Chem. Mater.* **14** 2270
19. Guo Z S, Zhao L, Pei J, Zhou J L, Gibson G, Brug J, Lam S and Samuel S M 2010 *Macromolecules* **43** 1860
20. Roncali J 1997 *Chem. Rev.* **97** 173
21. Barbarella G, Melucci M and Sotigu G 2005 *Adv. Mater.* **17** 1581
22. Kim J H and Lee H 2003 *Synth. Met.* **139** 471
23. Egbe D A M, Kietzke T, Carbonnier B, Muhlbacher D, Horhold H H, Neher D and Pakula T 2004 *Macromolecules* **37** 8863
24. Kiran A J, Udayakumar D, Chandrasekharan K, Adhikari A V and Shashikala H D 2006 *J. Phys. B: At. Mol. Opt. Phys.* **39** 3747
25. SujithKumar G and Tarasankar P 2007 *Chem. Rev.* **107** 4797
26. Venkatram N, Rao D N and Akundi M A 2005 *Opt. Express* **13** 867
27. Philip R, Ravindrakumar G, Sandhyarani N and Pradeep T 2000 *Phys. Rev. B.* **62** 13160
28. Gayvoronsky V, Galas A, Shepelyavyy E, Dittrich T, Timoshenko V Y, Nepijko S A, Brodyn M S and Koch F 2005 *Appl. Phys. B* **80** 97
29. Chen X, Zou G, Deng Y and Zhang Q 2008 *Nanotechnology* **19** 195703
30. Boyd R W, Gehr R J, Fischer G L and Sipe J E 1996 *Pure. Appl. Opt.* **5** 505
31. Takele H Greve H, Pochstein C, Zaporojtchenko V and Faupel F 2006 *Nanotechnology* **17** 3499
32. Neeves A E and Birnboim M H 1988 *Opt. Lett.* **13** 1087
33. Porel S, Venkataram N, Rao D N and Radhakrishnan T P 2007 *J. Appl. Phys.* **102** 33107
34. Gao Y, Tonizzo A, Walser A, Potasek M and Dorsinville R 2008 *Appl. Phys. Lett.* **92** 33106
35. Karthikeyan B, Anija M and Philip R 2006 *Appl. Phys. Lett.* **88** 53104
36. Sih B C and Wolf M O 2005 *Chem. Commun.* 3375
37. Hu X Y, Jiang P, Ding C Y, Yang H and Gong Q H 2008 *Nat. Photonics.* **2** 185
38. Hu X, Zhang J, Yang H and Gong Q 2009 *Opt. Express* **17** 18858
39. Chen X, Tao J, Zou G, Zhang Q and Wang P 2010 *Appl. Phys. A.* **100** 223
40. Zhong Q T and Tour J M 1998 *J. Am. Chem. Soc.* **120** 5355
41. Sheik-Bahae M, Said A A, Wei T H, Hagan D J and Van Stryland E W 1990 *IEEE J. Quantum Electron* **26** 760
42. Music S, Gotic M, Ivanda M, Popovic S, Turkovic A, Trojko R, Sekulic A and Furic K 1997 *Mater. Sci. Eng. B.* **47** 33
43. Zhu Y, Xu S, Jiang L, Pan K and Dan Y 2008 *React. Funct. Polym.* **68** 1492
44. Yang S H, Rendu P L, Nguyen T P and Hsu C S 2007 *Rev. Adv. Mater. Sci.* **15** 144
45. De Leeuw D M, Simenon M M J, Brown A B and Einerhand R E F 1997 *Synth. Met.* **87** 53
46. Joshi H S, Jamshidi R and Tor Y 1998 *Angew. Chem. Int. Ed.* **38** 2721
47. Gunter W and Stiles W S 1982 *Color science: Concepts and methods, quantitative data and Formulae*, 2nd ed. (New York: John Wiley and Sons)
48. Cassano T, Tommasi R, Tassara M, Babudri F, Cardone A, Farinola G M and Naso F 2001 *Chem. Phys.* **272** 111
49. Davies B L and Samoc M 1997 *Curr. Opin. Solid State Mater. Sci.* **2** 213
50. Venkatram N, Rao D N, Giribabu L and Rao S V 2008 *Chem. Phys. Lett.* **464** 211
51. Samoc M, Samoc A and Davies B L 1988 *Opt. Lett.* **23** 1295
52. Venkatram N, Naga Srinivas N K M and Rao D N 2002 *Chem. Phys. Lett.* **361** 439
53. Hegde P K, Adhikari A V, Manjunatha M G, Suchand Sandeep C S and Philip R 2011 *Adv. Polym. Tech.* **30** 312